ELSEVIER

Journal of Hazardous Materials 37 (1994) 285–302

JOURNAL OF HAZARDOUS MATERIALS

Reactive chemicals hazard evaluation: Impact of thermal characteristics of transportation/storage vessels†

Holly D. Ferguson*, Donald I. Townsend, Thomas C. Hofelich, Patrick M. Russell

Engineering Research and Process Development (HDF, DIT, PMR), Analytical Sciences (TCH), The Dow Chemical Company, Midland, MI 48667, USA

(Received 1 March 1993; accepted in revised form 28 October 1993)

Abstract

Runaway reactions occur when the total rate of heat generated in a system exceeds the rate of heat loss by the system. The major source of heat generation is by chemical reaction; this can be quantified calorimetrically, for instance via accelerating rate calorimetry. A review of the theory of adiabatic calorimetry and its application to thermal stability analysis is presented, focusing on simple reactive chemicals safety criteria that can be applied to vessels containing potentially hazardous materials. Heat losses from a given vessel can be determined by filling it with a hot, non-reactive fluid and then measuring the temperatures inside and outside of the vessel as it cools down. Results from a cool-down experiment on a 20000 gallon (75.7 m^3) insulated railcar are presented. Additionally, the efficacy of removing heat from the railcar via either hosing it with cooling water or by circulating cooling water in the car's heat exchange coils was evaluated. Time constants were determined for a series of different sized vessels, including the railcar. Large vessels have significant thermal inertia and can be poorly mixed (the latter resulting in thermal stratification). Ramifications of this are discussed, both for the routine handling of potentially hazardous materials and for emergency response if an accident were to occur. Runaway reactions were simulated by combining chemical reactions with vessel thermal characteristics with reactions in a model of the time-dependent temperature behavior of the system.

1. Introduction

Runaway reactions are composed of two parts – heat generation and heat loss. A runaway reaction occurs when the rate of heat generation exceeds the rate of heat loss. Heat generation can arise from an external source, such as a fire, and/or from an

* Corresponding author; send to: Dow Chemical Company, 734 Building, Midland, MI 48667, USA. Tel.: 1-517-638-1370.

† Presented at the AIChE 1992 Summer National Meeting, Hyatt Regency Minneapolis, Minneapolis, MN, paper #99b.

SSDI 0304-3894(93)E0107-D

internal source, for instance from a chemical reaction. Heat generation rates resulting from chemical reaction are routinely measured or calculated using differential scanning calorimetry (DSC), accelerating rate calorimetry (ARC), heat flow calorimetry, and other adiabatic or non-adiabatic methods.

Typically, kinetics determined by performing adiabatic experiments are combined with heat transfer information and then extrapolated to non-adiabatic, real, systems for thermal hazard evaluation. The theory of adiabatic calorimetry and its application to thermal stability analysis has been presented elsewhere [1–5]. The development below is intended to summarize the key aspects, focusing on presenting simple reactive chemicals safety criteria that can be used for vessels containing potentially hazardous materials. The impact of the assumptions and approximations made must be carefully considered when applying these results.

1.1. Self-heat rate and time to maximum rate (adiabatic systems)

Commonly , the rate constant for a chemical reaction increases exponentially with temperature, exemplified by the Arrhenius expression

$$k = A\mathrm{e}^{-E/RT} \tag{1}$$

For an nth-order reaction, a rate law can be defined as

$$\frac{\mathrm{d}C}{\mathrm{d}t} = -kC^n \tag{2}$$

or, for a pseudo-zero-order reaction (i.e. order equals zero or $n = 0$)

$$\frac{\mathrm{d}C}{\mathrm{d}t} = -k_\psi \tag{3}$$

where $k_\psi = kC_0^n$.

The concentration of C at temperature T in a reacting adiabatic system can be approximated by

$$C = \frac{T_\mathrm{f} - T}{\Delta T_{\mathrm{AB}}} C_0 \tag{4}$$

where T_f is the final temperature of the system and ΔT_{AB} is the adiabatic temperature rise

$$\Delta T_{\mathrm{AB}} = \frac{-\Delta H_r C_0 V}{\overline{mC_p}} \tag{5}$$

where $\overline{mC_p}$ is the average heat capacity of the system (including the vessel, reactants, products, inerts).

Differentiating Eq. (4) with respect to time and substituting the result into Eq. (2) gives the following self-heat rate

$$\frac{dT}{dt} = k\left(\frac{T_f - T}{\Delta T_{AB}}\right)^n \Delta T_{AB} C_0^{n-1} \tag{6}$$

Under initial conditions this reduces to

$$\left(\frac{dT}{dt}\right)_{T_0} = k\Delta T_{AB} C_0^{n-1} \tag{7}$$

The time required for a reaction to reach maximum rate, TMR, (although it may or may not indicate the time to explosion) is an approximate measure of the time available to respond to an emergency. TMR can be determined directly via experimentation, e.g. from ARC data (although a thermal inertia correction may be necessary for extrapolation). Alternatively, it can be estimated analytically. For a reaction with a relatively high activation energy it has been shown [4] that the time to maximum rate can be approximated by

$$\text{TMR} \simeq \frac{RT^2}{(dT/dt)E} \tag{8}$$

In an adiabatic system, the heat generation rate is equal to the rate of internal energy accumulation, which gives

$$\frac{dT}{dt} = \frac{-\Delta H k_\psi V}{\overline{mC_p}} \tag{9}$$

Substituting Eq. (9) into Eq. (8) gives an expression that can be used to estimate TMR [1]

$$\text{TMR} \simeq \frac{\overline{mC_p} RT^2}{-\Delta H k_\psi VE} \tag{10}$$

1.2. Thermal hazard evaluation – non-adiabatic systems

Thermal hazard evaluation requires knowledge of both the rate of heat generation and the rate of heat loss to or gain from the surroundings. Determination of heat generation and heat loss separately, and then combining this information to assess the hazard, avoids the danger and cost associated with performing full-scale runaway reactions. Heat generation is due to chemical reaction, as discussed above. Heat loss rates can be obtained either from experiments, from a heat loss model, or from a combination of the two. Some heat loss rate data are available for process equipment, but heat loss rates are less well known for storage or transportation containers – for instance drums, tank trucks, railcars, and barges. Inadvertent runaway reactions in transportation containers can have serious consequences, exacerbated by their large size and often remote location.

Heat loss (or gain) can result from a number of sources including heat flow (a) from vessel jacketing; (b) through the vessel surface; (c) from the sun's radiation; (d) from addition or removal of material from the vessel; (e) from agitation; and (f) from physical phenomena such as evaporation, crystallization, or mixing. Kumana and Kothari [6] present a detailed analysis of heat flow owing to (a–c), assuming a uniform internal temperature. They do not consider the transient case. Bourne and coworkers [7, 8] studied heat flow from a vertical unstirred vessel (with an adiabatic lid and isothermal walls having a uniform heat transfer coefficient), obtaining the temperature distribution inside the vessel as a function of time.

In this analysis, heat loss to or gain from the environment will simply be modelled as a heat transfer coefficient, U, multiplied by a heat exchange area, a, and then multiplied by a temperature driving force. The temperature driving force will be approximated by the difference between an average internal temperature, T, and an average ambient temperature, T_A. A heat balance, for the case of a zero-order reaction, gives that the heat generation rate equals the thermal energy accumulation rate plus the heat loss rate

$$-\Delta H k_\psi V = \overline{mC_p}\frac{dT}{dt} + Ua(T - T_A) \tag{11}$$

Fig. 1 plots the heat generation rate and the heat loss rate versus internal temperature. At steady state, dT/dt is zero and the rate of heat generation equals the rate of heat loss (points A and B for the upper heat loss line). Point A is a stable steady-state point: if the system is perturbed to a temperature above or below point A, the system will relax to point A. Point B in Fig. 1 is a metastable steady-state point: if the internal temperature drops just slightly, the heat loss rate will be greater than the heat generation rate and the internal temperature will decrease to point A. However, if the internal temperature is perturbed above point B, a thermal runaway will occur.

At the critical point ($T = T_{NR}$), the slope of the heat generation line equals the slope of the heat loss line (point C). Point C may be obtained by increasing the ambient temperature (as shown by the dashed line) or by decreasing the heat transfer rate (reducing the slope of the heat loss line). At point C, any increase in temperature or decrease in heat loss will result in a runaway.

The thermal time constant of the vessel can be found by setting the heat generation rate in Eq. (11) to zero and rearranging

$$\tau_v = \frac{\overline{mC_p}}{Ua} = \frac{-(T - T_A)}{dT/dt} \tag{12}$$

Substituting dT/dt from Eq. (7) into Eq. (12) and then taking the derivative with respect to temperature gives

$$\mathrm{TMR}|_{T_{NR}} = \frac{\overline{mC_p}}{Ua} \tag{13}$$

In other words, the TMR at T_{NR} equals the time constant of the vessel. Note that this is an approximate result derived from substituting the adiabatic rate of temperature

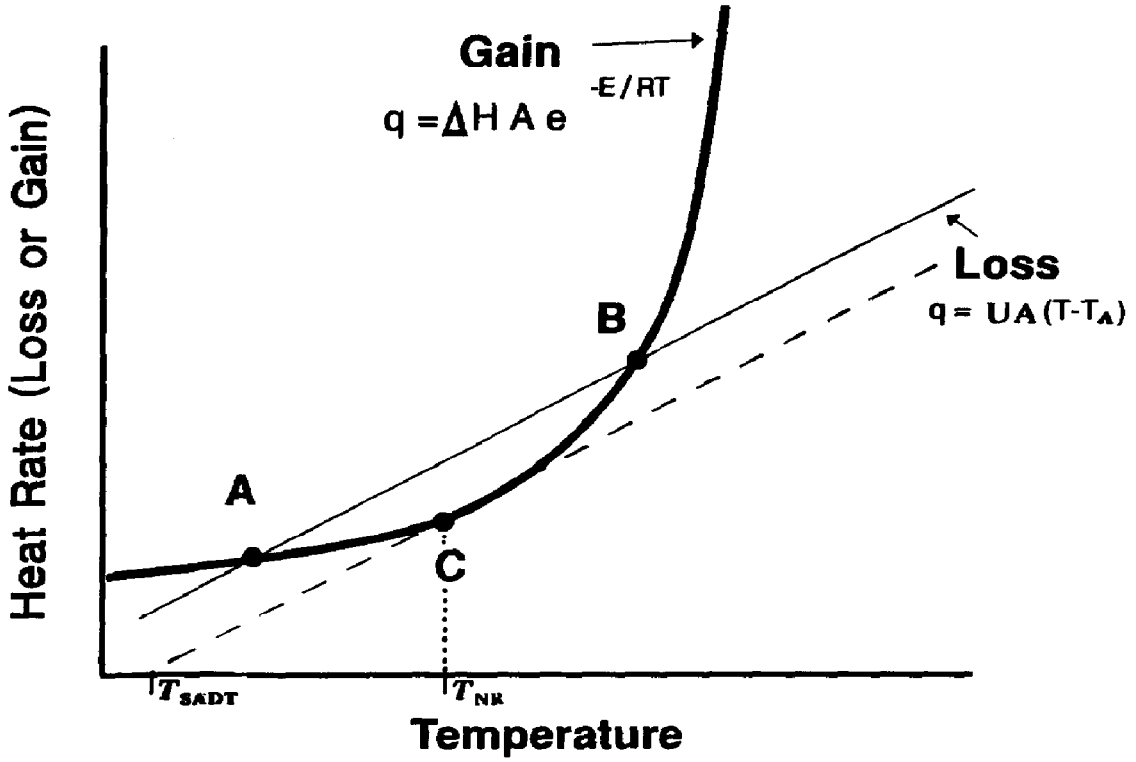

Fig. 1. The self-heat rate and heat transfer rate as a function of temperature.

increase under initial conditions into the steady-state heat balance. This approximation is better when T is close to T_A, in the early stages of a runaway, and for nearly adiabatic systems.

Equating the above equation with Eq. (10) gives an expression useful for estimating T_{NR}

$$T_{NR}^2 = \frac{-\Delta H k_\psi V E}{UaR} \tag{14}$$

The so-called self-accelerating decomposition temperature, T_{SADT}, is defined as the minimum external (ambient) temperature at which a given vessel or container will decompose in seven days or less. T_{SADT} can be calculated from T_{NR} as follows [1]

$$T_{SADT} = T_{NR} - \frac{RT_{NR}^2}{E} \tag{15}$$

1.3. Approach

The heat loss/gain characteristics of a vessel can be estimated via Eq. (12), calculated via the method described by Kumana and Kothari [6], or determined experimentally. Numerical estimates are complicated by the fact that heat loss to gain from the environment frequently involves multiple, interacting heat flow paths

combined with non-uniform internal and ambient temperature distributions. On the other hand, passive (e.g. with no reaction occurring) experiments can be performed under conditions closely simulating the real, active system.

Passive experiments involve filling a vessel with a hot, non-reactive fluid (such as water), then observing the internal temperature decay over time [1, this work]. τ_v for the active system can then be calculated as follows

$$\tau_{\text{active}} = \frac{(\overline{mC_p})_{\text{active}}}{(\overline{mC_p})_{\text{passive}}} \tau_{\text{passive}} = \frac{(\overline{mC_p})_{\text{active}}}{(Ua)_{\text{passive}}} \tag{16}$$

where τ_{passive} is the experimentally determined time constant for the passive system (using the integrated form of Eq. (12)). In addition, it is important to determine how well mixed the vessel's contents are. A single hot spot in which a runaway reaction is occurring can result in the entire contents of the vessel running away unless countermeasures are taken. Temperature measurements in various positions within a vessel during the cool-down can help in estimation of vessel mixedness in an emergency situation.

In this work, three experiments were done, determining:

(1) the cool-down rate from a stationary, indoor, railcar;
(2) the efficacy of hosing down the railcar with cold water for removal of heat; and
(3) the efficacy of circulating cold water through the heating coils as a means to remove heat.

2. Experimental

Experiments were conducted from mid-August to mid-September, 1991 on a 20000 gallon (75.7 m^3) insulated rail tank car (manufactured by Union Tank Car Co., Fig. 2). This type of tank car is representative of over 60% of Dow Chemical's liquid rail transportation fleet. The car is approximately 44 ft (13.4 m) long, and 10 ft (3.05 m) in diameter. It is fabricated of mild steel, has no lining material on the interior, and is insulated with four inches (0.102 m) of mineral wool.

On 22 August 1991 between 5 and 6:45 pm, the car was filled with 82 °C (180 °F) water until hydraulically full (168100 lbs water) via a dip pipe that discharged near the bottom middle of the car. A standpipe in the top of the car was left open to the atmosphere to allow for thermal expansion. The car was parked inside a tank car washing facility (at Dow Chemical's Midland site). Care was taken to limit the air circulation by closing the overhead doors near the car. On 9 September 1991 (3 pm), the car was moved outside. The firehosing experiment was done the next day. Cooling water was run through the external coils beginning on 12 September 1991 at 9:20 am, while the car was still outside.

Thermal data were obtained by observing the temperature inside the car decay over time. Both internal and external temperatures were measured. To assess the degree to which the water was thermally mixed, the water temperature was measured at various positions inside the railcar using type J thermocouples (Fig. 2). Temperatures were

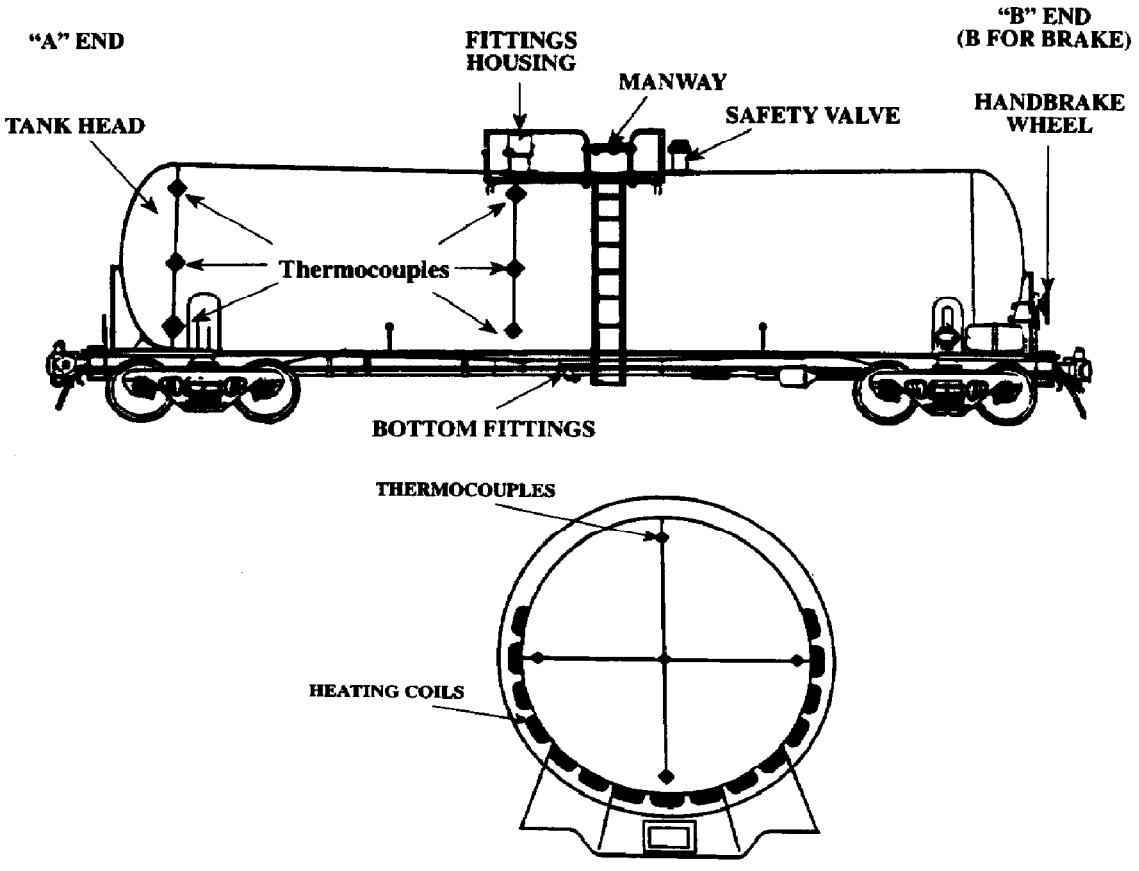

Fig. 2. Schematics of a rail tank car, giving internal thermocouple positions. The top schematic gives a side view, while the bottom schematic gives an end view. The placement of the heating coils can be seen in the bottom drawing.

measured with an array of thermocouples placed in the middle and in the front or A-end of the car.

Each array had probes in the center and one foot from the top, bottom, and sides of the car. Thermocouples for measuring external temperatures were placed on the tank's surface. Additional thermocouples were placed at 1 and 2.5 ft (0.3 and 0.76 m) from the tank surface to measure the air temperature near the tank. The data were recorded, every hour for the first day and less frequently later on, using a Hewlett-Packard 85 computer with a Hewlett-Packard 3279 data logger.

3. Results and discussion

3.1. Surface temperatures and thermography

The loss of heat from the car was immediately obvious in that the air surrounding the car was hotter than ambient. On the second day of the cool down,

a thermographic camera was used to measure surface temperatures. Much of the car's outer surface was at close to ambient temperature, indicating that the insulation provides the limiting resistance for heat transfer in those regions. Some downwards slippage and some separation of the insulation was evident. In contrast, some areas were significantly hotter than ambient; in many cases these were areas where components were welded directly to the internal steel tankage. Examples include the brake assembly, the bolsters and chassis, the manway, the valve and dip pipe assembly, and the piping for the heat exchange coils and the bottom drain. Some of these temperatures were as little as 10 °C below the internal temperature.

3.2. Cooldown profiles

Figs. 3 and 4 give thermal decay profiles for the A-end and the middle of the car, respectively. After nearly three weeks, only about 20 °C have been lost, corresponding to a temperature fall off of about 1 °C per day at a temperature difference (internal minus external) of roughly 30 °C. Approximately five days are required for the system to reach "steady state". During this transient period, the car's metal warms up quickly, cooling the water near the walls. Then this cooler water is gradually warmed by the more interior water. The end result is that A-end (about one foot from the wall) temperatures actually rise for several days before beginning to decline.

The temperature in the middle of the car begins at about 78 °C, close to the temperature of the water with which the car was initially filled. However, the bottom temperature declines rapidly, eventually establishing about a 20 °C gradient from the center to the bottom. Water near the walls is cooled and "slides" down the walls to pool in the bottom. No vertical thermal gradients are observed in the top half of the

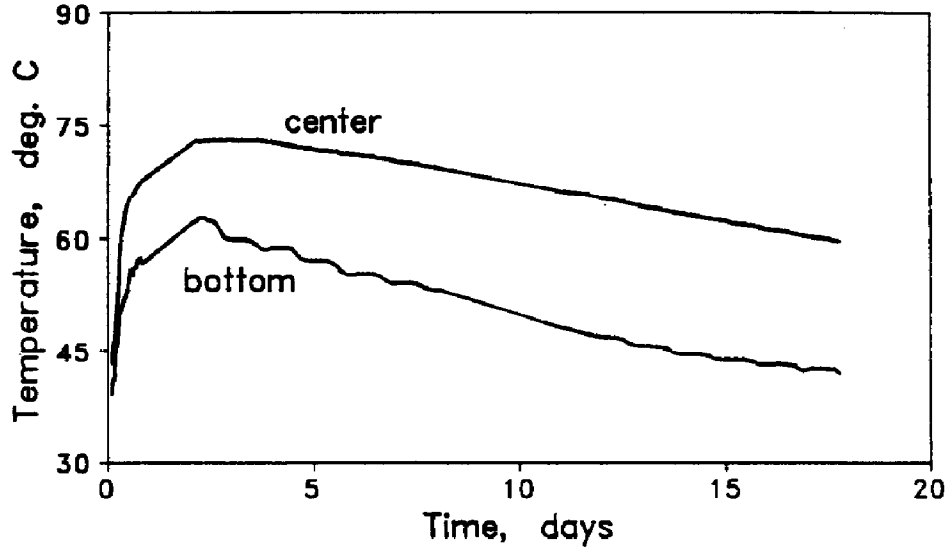

Fig. 3. Thermal decay of an insulated railcar: A-end.

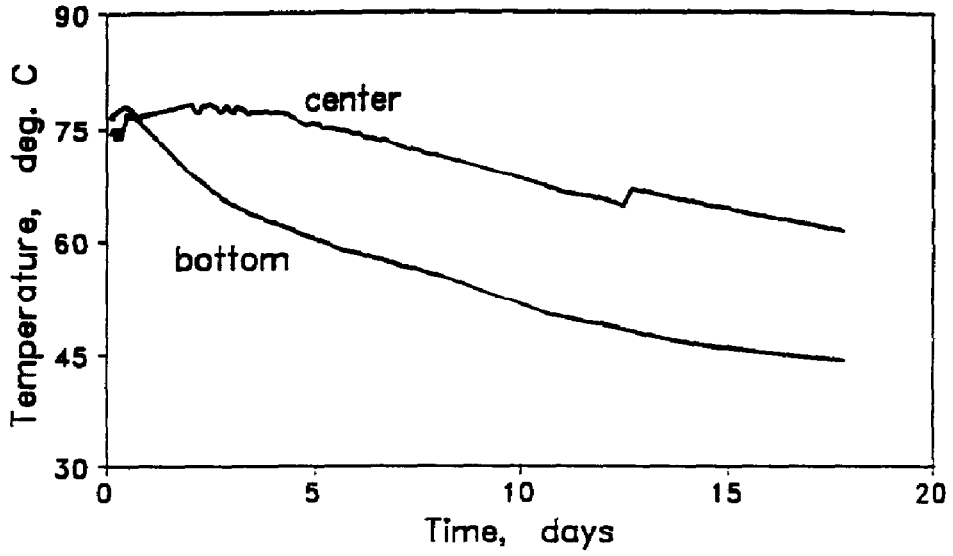

Fig. 4. Thermal decay of an insulated railcar: middle.

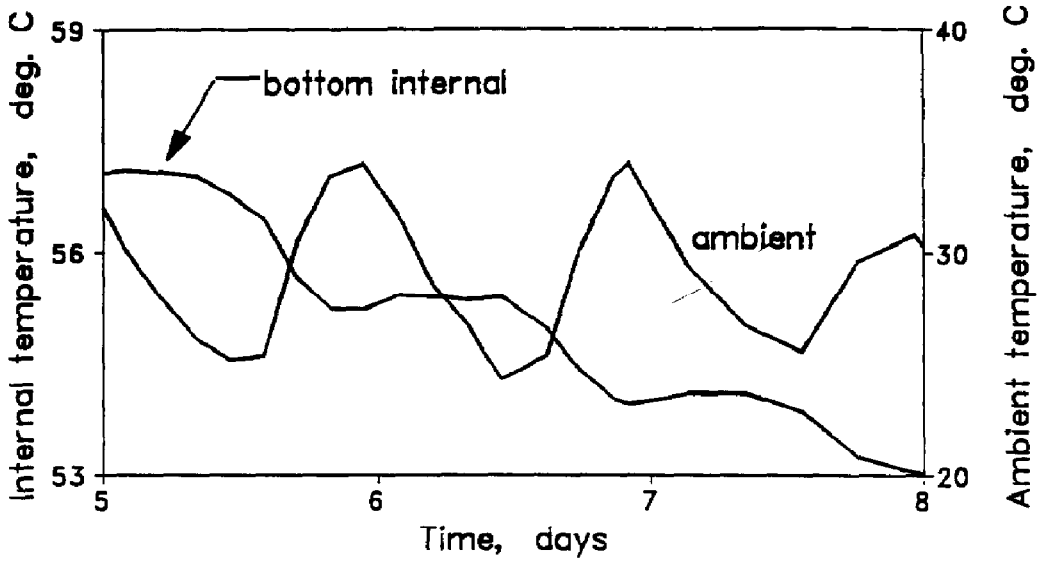

Fig. 5. Thermal decay of an insulated railcar: day/night oscillations in the A-end bottom internal temperature.

car perhaps since the water near the walls that is cooled "falls" straight down rather than "slides" down the walls.

After the thermal gradient is set up, the bottom and the center temperatures in both the A-end and the middle of the car decline nearly in parallel, both losing about 1 °C per day. A slight horizontal gradient is set up, with the A-end maintaining a slightly lower temperature than the middle. As the car cools, its internal temperature is

approaching the ambient temperature; this results in the observed curvature in the cool-down profiles.

Note that the A-end bottom temperature oscillates in a regular fashion, while the other temperature profiles are relatively smooth. This oscillation is diurnal, resulting from fluctuations in the ambient temperature. A significant amount of the heat lost from the car in this region flows through uninsulated regions and appendages. These regions are less thermally isolated from the environment. Fig. 5 plots the A-end bottom internal temperature along with the ambient temperature. Day/night fluctuations of about 10 °C in the ambient temperature were observed. The oscillations in the internal temperature are time-delayed behind the ambient temperature oscillations by about 10 h and have an amplitude of only about 0.5 °C. In contrast to the oscillatory pattern observed in the A-end bottom internal temperature profile, ambient temperature oscillations are damped out in other regions of the car, where heat flow out is more dominated by the higher-time-constant process of heat flow through the insulation.

3.3. Emergency response

What is the appropriate response to make in the event of a potential reactive chemicals emergency? Possible responses include: hose the car with water, dilute (and thereby cool) the contents of the car, use the heat exchange coils that are normally used to heat the car for cooling, move the car to a remote site, and if the situation merits, simply get people away from the emergency site.

3.3.1. Firehosing

Firehosing is used to knock down hazardous vapors, to maintain the car's walls cool in the event of fire impingement (to maintain the integrity of the car's walls), and to cool the car's contents. Water is typically placed on the top of the car and allowed to run down the sides. How effective is this in cooling the car?

About 10000 gallons (37.85 m^3) of water were sprayed for about an hour onto the upper portion of the car using a monitor cannon. Firehosing had little effect on the internal temperatures (Fig. 6). The top and center temperatures dropped about 1 °C during the hosing, while the left side and the bottom temperatures actually rose by about the same amount, indicating a shifting in the internal free convection pattern. The observed cool-down rate during the hosing was enhanced only moderately (about twofold), owing to an increase in the external heat transfer coefficient on the uninsulated and poorly insulated regions.

3.3.2. Heat exchange coils

Many railcars have heat exchange coils, typically used for heating. Could these coils be used to cool a railcar in an emergency situation? As seen in Fig. 2, these coils are in intimate contact with the lower half of the railcar's tank. Cooling water (from a fire hydrant) was connected to the coils and the inlet and outlet temperatures recorded over a 3.5 day test. The water flow rate and temperature were about 45 gpm (0.00284 m^3/s) and 22 °C, respectively.

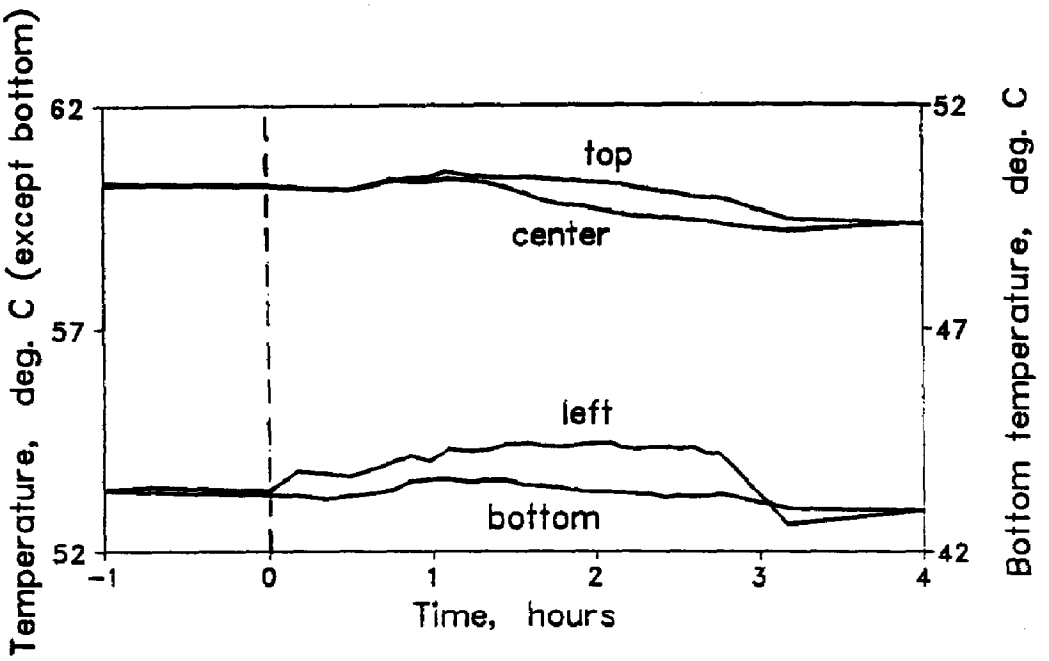

Fig. 6. The effect of hosing a railcar with cooling water on the middle internal temperatures.

Much of the heat is removed from the car over the first 10 h (Fig. 7). After about 20 h, the inlet and outlet temperatures are almost the same, indicating only a slow removal of heat. The center and bottom thermocouples inside the railcar show a rapid 2 °C loss in temperature per hour initially (Fig. 8). This is about 24-fold the rate at which the railcar dropped in temperature during the cool down with just air in the coils. Even at this fast cooling rate, it takes about a day to drop those temperatures to close to the temperature of the cooling water. The cooling rate in the portion of the car was increased about two-fold, probably owing to an increase in the temperature driving force for heat conduction. Measurements with a portable thermocouple indicated that while the top 2 ft (0.61 m) were isothermal and hot, the bottom 5 ft (1.52 m) were also nearly isothermal (but were cool). Between a depth of 2 and 3 ft (0.61 and 0.91 m), a steep isotherm, spanning nearly 30 °C, had developed.

When the coils are used for heating, the resulting density gradients promote mixing via free convection. When these same coils are used for cooling, a stable density gradient is produced. Efficient removal of heat from the top portion of the car requires an alternative means of mixing the car's contents, for instance moving or "jockeying" the car, recirculating the car's contents, or sparging gas. Alternatively, if the coils encompassed the entire circumference of the tank, they would be effective for both heating and cooling.

3.4. Application of results

The time constant for the railcar during the cool down $\tau_{passive}$, was estimated to be 31 days. This gives a U of 1.0 W/m^2 °C (using a surface area of 116 m^2). If the railcar

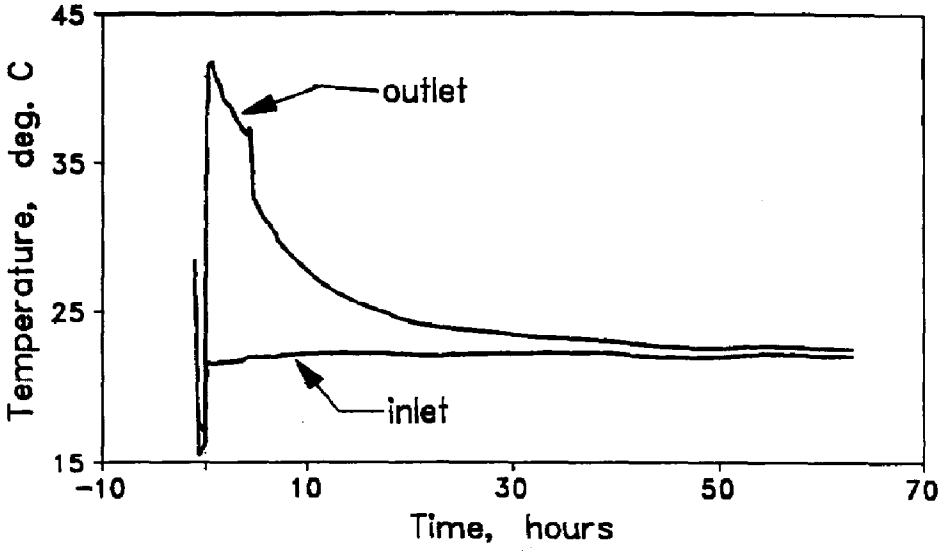

Fig. 7. The effect of cooling a railcar with the heat exchange coils: temperatures at the inlet and outlet of the coils.

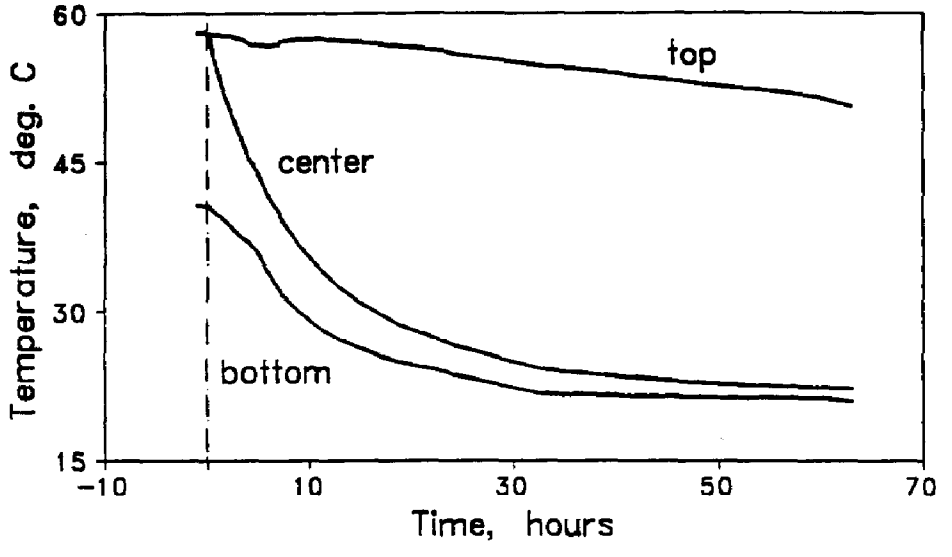

Fig. 8. The effect of cooling a railcar with the heat exchange coils: middle internal temperature profiles over time.

were completely insulated, the heat flow from it would be limited by the conductivity of the insulation (times the surface area). If this were true, U would equal the thermal conductivity of the insulation divided by the insulation thickness. From this analysis, it was determined that roughly half of the heat loss from the car flowed through the insulation while the remainder flowed through the poorly and non-insulated regions.

Table 1
Heat transfer data for different vessels. Data were obtained from cool-down experiments with water. τ is $\tau_{passive}$. Details concerning the vessels: flask: 1-l round-bottom, glass; 55 gallon (0.21 m^3) drum, steel; tank truck: two compartments of a three-compartment tank, each holding 2500 gallons (9.46 m^3); storage tank: one compartment of two-compartment horizontal cylindrical steel tank with one inch of fiberglass insulation, each compartment holding 10000 gallons (37.85 m^3) and 12 ft (3.66 m) diameter by 13 ft (3.96 m) long; railcar: 20000 gallons (75.7 m^3) capacity, with 4 in (0.102 m) of insulation, as described in this work

Vessel	Mass of water (kg)	τ (days)	U ($W/m^2\,°C$)
Flask	1	0.076	12
55 gallon drum	220	0.42	8.5
Tank trunk	19,700	2	6.8
Storage tank	42,700	12	2.7
Railcar	76,000	31	1.0

If U were assumed to be that of the insulation (neglecting the importance of losses through the metal appendages and other non-insulated surfaces) for thermal hazard evaluation, an overly conservative estimate of safety would result.

Passive, cool-down experiments have been run on other vessels, including lab glassware, unstirred pilot-plant reactors, a drum, a tank truck, a 10000 gallon (37.85 m^3) insulated tank [9]. Table 1 gives $\tau_{passive}$ (for water) and U values for some of these vessels.

As the vessel time constant increases, the associated maximum heat generation rate that can be tolerated before a runaway reaction occurs decreases. The maximum tolerable heat generation rate in the railcar studied in this work corresponds to a temperature rise of order 1 °C/day. This is well beyond the sensitivity of the ARC (0.02 °C/min or 29 °C/day). Hence either ARC data are extrapolated (assuming no change in mechanism at the lower temperature) or more sensitive calorimetry is required. For example, isothermal heat flow calorimeters could be used to provide data at very low heat generation rates [10–12].

Fig. 9 gives a comparison of heat rate versus the temperature at which the exotherm was detected for a range of calorimeters. When choosing a calorimetric technique with which to obtain heat generation data, consideration must be given not only to the chemical system of interest, but also to the accuracy of the data required, the calorimeter's sensitivity (as compared to τ_{active}), the amount of mixing the calorimeter provides, and the validity of data extrapolation.

Equipment time constants can be directly used in thermal hazard evaluation. Take as an example, the case of a railcar filled with uninhibited styrene. $\tau_{passive}$ for the railcar was 31 days, from which τ_{active} was calculated via Eq. (16) to be 13.5 days. The adiabatic TMR was then calculated via Eq. (10) and the styrene properties given in Table 2. A plot of TMR versus temperature shows that T_{NR}, estimated to be the

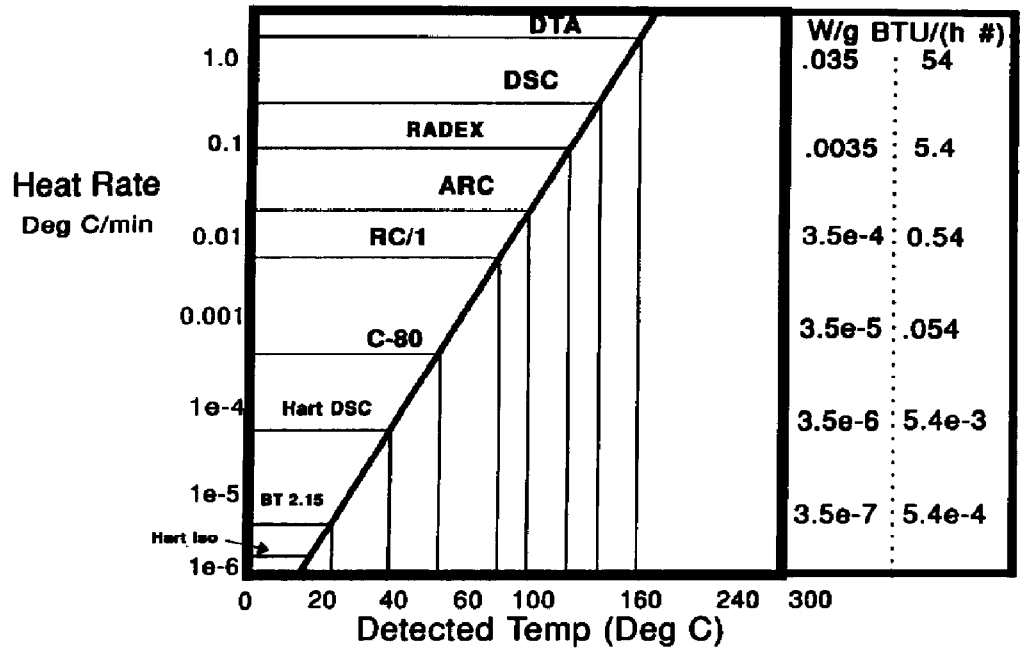

Fig. 9. Comparison of sensitivities of different calorimeters. DTA: differential thermal analysis (DuPont), DSC: differential scanning calorimeter (DuPont), RADEX: (ASTRA Scientific), ARC: accelerating rate calorimeter (Columbia Scientific Industries), RC/1: RC1 reaction calorimeter (Mettler Instrument Corp.), C80: heat flow calorimeter (Setaram), BT2.15 heat flow calorimeter (Setaram), Hart Iso: isothermal DSC (Hart Scientific). For a zero order reaction, $E = 20$ kcal/mol. Numbers obtained from a nominal sample loading and five times the baseline RMS noise taken as the minimum detectable signal, either as stated by the manufacturer where available, or measured.

Table 2
Properties of styrene used in thermal runaway simulation. Kinetic constants are from Ref. [13]

$\log k_\psi = a + b/T$ (wt. polymer/h)	m (kg)	ΔH (kcal/mol)	C_p (cal/g °C)
$a = 11.55$, $b = 4170$	76000	14.9	0.5

temperature at which the TMR equals τ_{active} via Eq. (13), is about 36 °C (Fig. 10). The same result for T_{NR} is obtained if Eq. (14) is used. From the T_{NR}, a self-accelerating decomposition temperature, T_{SADT}, of about 20 °C is obtained via Eq. (15).

A better estimate of TMR and T_{NR} can be obtained by performing a transient heat balance, considering the heat loss from the railcar in addition to the heat gain resulting from the styrene polymerization (Eq. (11)). Simulations of internal temperature as a function of time were then made for different ambient temperatures using Dow Chemical's *SimuSolv*™ computer program. No credit was taken for evaporation of the styrene monomer or small oligomers. The initial temperature of the contents

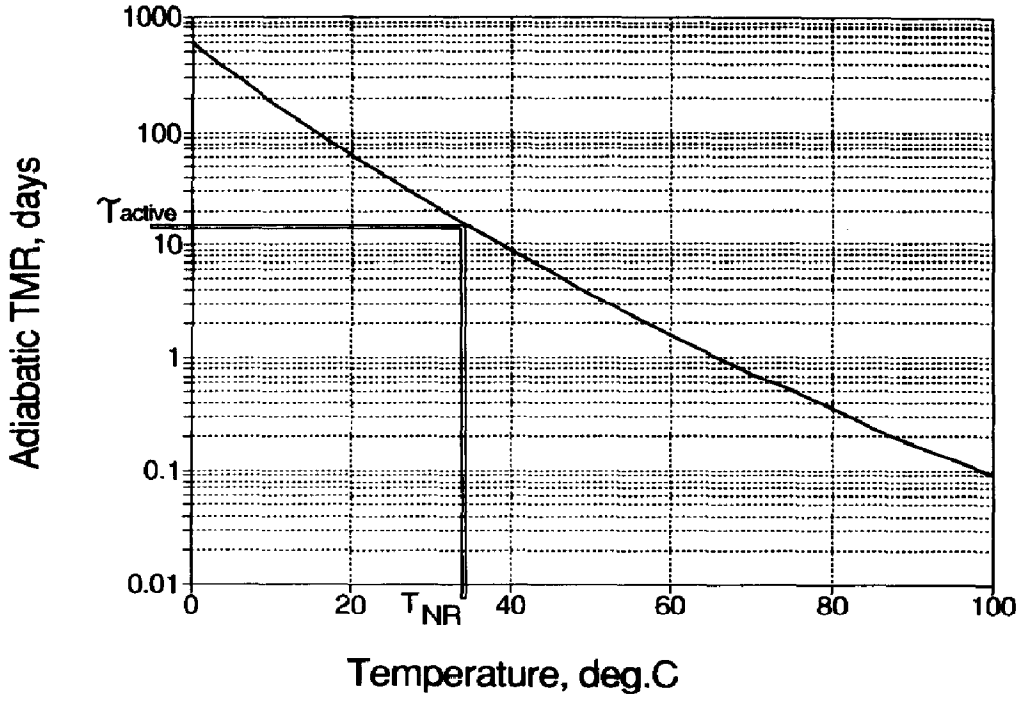

Fig. 10. Adiabatic TMR versus temperature for the case of a railcar filled with uninhibited styrene.

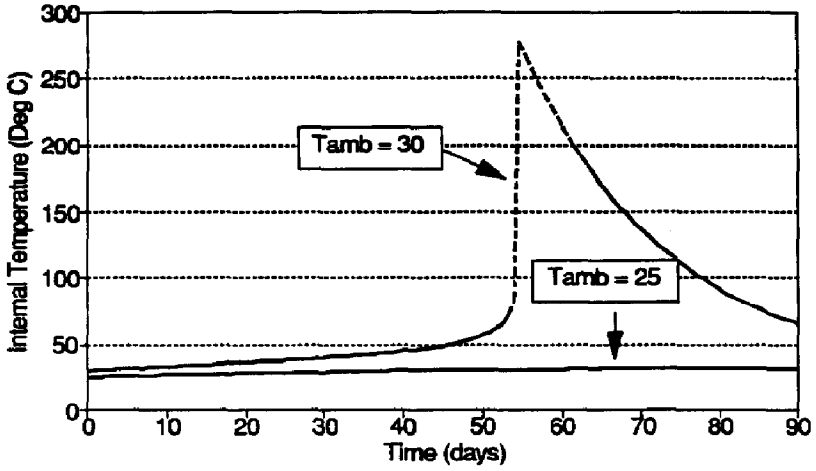

Fig. 11. Runaway simulation in a railcar filled with uninhibited styrene: internal temperature profile versus time for ambient temperatures of 25 °C and 30 °C.

was set equal to that of the environment and both the internal and the ambient temperatures were assumed to be uniform. Fig. 11 gives representative results, at ambient temperatures of 25 and 30 °C. Note that while the styrene will never run away in the 25 °C case, an increase of 5 °C increases the ambient temperature above T_{SADT} and a runaway reaction occurs. The estimate for T_{SADT}, when heat losses are

accounted for, is, as expected, less conservative than when no heat losses were assumed (25–30 °C versus 20 °C). For the runaway case, note the long period of time over which the temperature rises only slightly, which is then followed by a rapid exotherm at about 55 days. The adiabatic TMR at 30 °C is similar but predictably more conservative: 23 days instead of 55 days.

The internal and external temperatures and the rate of internal temperature rise during a potential reactive chemicals emergency can be used directly in thermal stability analysis. If $(dT/dt)_{active}$ is greater than $(dT/dt)_{passive}$ (from Eq. (12)), there must be heat generation from reaction (if heat input from agitation, radiation, etc. are either negligible or are accounted for). If the activation energy is known or can be estimated, then TMR can be estimated from Eq. (8).

4. Conclusions

The key thermal property of a vessel is its time constant, τ_{active}. Knowledge of τ_{active}, combined with knowledge of the rates of heat generation (e.g. from the chemistry, agitation, etc.) allows one to estimate the time to maximum rate (TMR) and the temperature of no return (T_{NR}). TMR and T_{NR} can then be used to evaluate a potential hazard and to develop an emergency response plan. These parameters can be estimated via the relatively simple expressions presented above, or, alternatively, more accurate estimates can be obtained from simulations of the time-dependent mass and energy balances.

Large vessels and vessels that are used for transportation and storage have additional complexities. Significant thermal and chemical gradients may exist. In vessels with little or no instrumentation, thermography (and/or other surface temperature measurement techniques) could be used to aid in estimation of internal temperatures. Temperature indicating labels could be placed on all large vessels containing certain chemicals. Then routine checking of these temperatures could provide early warning that the contents of a car were heating up. Mixing a vessel's contents could be a very effective way to reduce the potential hazard. However, care must be taken with two-phase systems which require both phases to contact for reaction. Another complication is that heat loss to or gain from the environment can involve multiple paths. High heat flux paths provide efficient paths for vessel cooling; however, they also provide paths via which heat can be gained rapidly during an emergency, for instance in a fire situation.

The data and analysis presented in this work have application in Safety and Loss Prevention, Emergency Response, in transportation certification, and to optimize shipping conditions for thermally-sensitive materials. Current work is aimed at implementing improvements to the transient energy balance-based model to better address heat flow from radiation and the multiple paths for heat transfer with the environment. In addition, there is a need to study very large vessels and the impact of stratification.

5. Nomenclature

a	heat transfer area (dm^2)
A	kinetic pre-exponential factor

C	reactant concentration (mol/l)
C_0	initial concentration
E	kinetic activation energy (J/mol)
ΔH	heat of reaction (J/mol, (−) for exothermic)
k	reaction rate constant
k^*	pseudo-zero-order reaction rate constant (mol/l s)
mC_p	average (extensive) heat capacity (J/K)
n	reaction order
R	universal gas constant (8.32 J/mol K)
t	time (s)
T	internal temperature (K)
T_A	ambient temperature
ΔT_{AB}	adiabatic temperature rise (K)
ΔT_{max}	maximum temperature difference, $T - T_A$ (K)
T_f	final temperature (for an adiabatic thermal runaway)
TMR	time to maximum rate
T_{NR}	temperature of no return (K)
U	heat transfer coefficient (W/dm^2 K)
V	volume (l)
τ	time constant, subscripts as follows: v – time constant of the vessel, active – for the active (reactive) system, passive – for the passive (non-reactive) system.

6. Acknowledgements

The authors wish to acknowledge the help of Al Anderson, John Roper, the staff at the Railcar Wash facility, Mike Young, and Dow's Emergency Response Group and the Fire Department.

7. References

[1] H.G. Fisher and D.D. Goetz, Determination of self-accelerating decomposition temperatures using the accelerating rate calorimeter, J. Loss Prev. Process Ind., 4 (1991) 305–316.
[2] R.W. Gygax, Scale-up principles for assessing thermal runaway risks, Chem. Eng. Prog., (1990) 53–60.
[3] J.C. Leung, H.K. Fauske and H.G. Fisher, Thermal runaway reactions in a low thermal inertia apparatus, Thermochim. Acta, 104 (1986) 13–29.
[4] D.I. Townsend and J.C. Tou, Thermal hazard evaluation by an accelerating rate calorimeter, Thermochim. Acta, 37 (1980) 1–30.
[5] J.K. Wilberforce, Applications of the accelerating rate calorimeter in thermal hazards evaluation, Ind. Chem. Eng. Symp. Ser., 85 (1984) 329–343.
[6] J.D. Kumana and S.P. Kothari, Predict storage-tank heat transfer precisely, Chem. Eng., (1982) 127–132.
[7] J.R. Bourne, F. Brogli, F. Hoch and W. Regenass, Heat transfer from exothermically reacting fluid in vertical unstirred vessels. I. Temperature and flow fields, Chem. Eng. Sci., 42 (1987) 2183–2192.

[8] J.R. Bourne, F. Brogli, F. Hoch and W. Regenass, Heat transfer from exothermically reacting fluid in vertical unstirred vessels. II. Free-convection heat transfer correlations and reactor safety, Chem. Eng. Sci., 42 (1987) 2193–2196.
[9] T.C. Hofelich and H.D. Ferguson, 1991, unpublished.
[10] T. Hoppe and B. Grob, Heat flow calorimetry as a testing method for preventing runaway reactions, in: Int. Symp. Runaway Reactions, AIChE (1989) 132–154.
[11] L.G. Karlsen and J. Villadsen, Isothermal reaction calorimeters. I. A literature review, Chem. Eng. Sci., 42 (1987) 1153–1163.
[12] T.C. Hofelich, The use of calorimetry for studying the early part of potential thermal runaway reactions, in: Int. Symp. Runaway Reactions, AIChE (1989) 232–246.
[13] E.R. Moore, (General Editor), Encyclopedia of Polymer Science and Engineering, Vol. 16, Wiley, New York, 2nd edn., 1989, p. 25.